Imprecise random field analysis with parametrized kernel functions

Matthias Faes[a,*], David Moens[a]

[a]*KU Leuven, Department of Mechanical Engineering, Technology campus De Nayer, Jan De Nayerlaan 5, St.-Katelijne-Waver, Belgium*

Abstract

The application of isotropic random fields in engineering analysis requires the definition of their first two central moments, as well as their covariance function. In general, insufficient data are available to make a fully objective crisp estimate on these quantities, and hence, subjectivity enters implicitly into the analysis. The framework of imprecise probabilities is gaining popularity in this context, as it allows to explicitly separate the epistemic uncertainty, present due to data insufficiency, from the aleatory nature of the random parameters. However, an approach that is capable of handling imprecision in the complete definition of the imprecise random field is lacking to date. This paper proposes a framework for imprecise random field analysis with parametrized covariance functions. As such, the functional form of the covariance function is assumed to be known deterministically, whereas the governing parameters are subjected to imprecision. First, a comprehensive analysis of the effect of imprecise random fields, given imprecision on both the mean and auto-covariance structure, is presented. It is shown that the discretization of an imprecise random field, given interval-valued correlation lengths cannot be performed using interval arithmetical procedures as the resulting basis functions are in that case no longer a complete basis on $\mathcal{L}_2$. Therefore, an iterative procedure is proposed where the bounds on the imprecise random field basis are determined via an optimization procedure. This

*Corresponding author
Email address: matthias.faes@kuleuven.be (Matthias Faes)

procedure provides exact bounds on the response of a system in case the system is monotonic with respect to the random field realizations. Two illustrative case studies on a mass-damper-spring system and a dynamic state-space model of a car suspension are included to illustrate the methodology. These case studies illustrate that indeed a separation between aleatory and epistemic uncertainty is possible in random field analysis, and hence, more objective results are obtained at only slightly increased computational cost.
Keywords: imprecise probability, random field analysis, interval arithmetic, imprecise random fields, parametrised p-box, transient dynamics

---

1. Introduction

In the context of including non-determinism into numerical models, two complementary philosophies exist. Usually, either a probabilistic or a possibilistic (interval) approach for the representation of the variability and/or uncertainty is followed. Using the former class of methods, the non-determinism in the model parameters is represented using joint-probability density functions that assign a (relative) likelihood to different parameter values within a predefined interval. The latter approach considers only the crisp bounds between which the possible values of the corresponding parameter lie for analysis. This is sometimes also referred to as an uncertain-but-bounded representation of the uncertainty. A large body of literature has been dedicated to the comparison of both philosophies in a forward [1] (i.e., from parameters to model responses) and inverse (i.e., from responses to parameters) uncertainty quantification setting [2]. These studies show that, instead of conflicting, both approaches are complementary in a design context, and in fact the selection of the most appropriate approach should be based on the quantity and quality of information that is available to the analyst [3].

Special considerations however have to be made in case correlated multivariate parameters are considered. This, for instance, is highly relevant for the modeling and simulation of spatially uncertain model quantities (e.g., spa-

tially varying soil properties). The interval framework, while highly objective under scarce data, is less suited for the description of such multivariate non-deterministic quantities, as intervals are by definition independent. Therefore, the classical interval framework will be over-conservative in this context. Moreover, due to the lack of an interval measure for dependence, the description of spatial interval uncertainty proves to be a non-trivial task. Interval methods have been mainly applied in low dimension problems (see e.g. [4, 5]), but also some more realistic applications have been introduced so far [6, 7, 8], including crack propagation [9]. Also initiatives towards including interval analysis into commercial software have been undertaken [10]. Methods to cope with dependence in a multivariate interval context where only introduced very recently. For instance, Verhaeghe et al. was the first to introduce the interval field framework to model spatially dependent uncertainty in an interval context [11]. This work was later extended in the context of inverse dependent interval analysis in [12]. Furthermore, Sofi et al. introduced interval field analysis via Karhunen-Loève expansions and the improved interval analysis via the extra unitary interval [13, 14]. The authors recently introduced a generic framework for dependent interval analysis based on the admissible set decomposition which, similar to vine copula, decomposes the high-dimensional dependence between intervals at the input of a model into conditional and unconditional bi-variate admissible sets [15]. Finally, also fuzzy fields were introduced very recently [16]. Nonetheless, all these developments fail to give an analyst a highly informative description of the joint non-deterministic nature of the uncertainty at hand, as a convex set description of the non-determinism is obtained at best. Note that such description is often the most objective information that can be derived from data, especially when the data are scarce [2].

On the other hand, when sufficient data are available, the probabilistic framework is highly suited for the description of multivariate uncertain non-deterministic quantities, e.g. following a random fields approach [17], which are widely applied for spatial reliability analysis in domains such as material science [18], geology [19] or computational fluid dynamics [20]. In some cases, non-

probabilistic and probabilistic uncertainty are jointly present in the model under consideration. In this context, considerable work has also been performed in the efficient combination of probabilistic and interval uncertainty. For instance, Do et al. proposed a spectral stochastic method to propagate random fields together with intervals [21]. Wu et al. proposed to propagate a combination of random and interval fields using a framework called extended unified stochastic sampling, which combines regular sampling methods with interval analysis [22]. Zheng et al. developed a robust Topology Optimization scheme under hybrid uncertainty [23]. Finally, Faes et al. applied a combination of random field and interval field analysis to study the reliability of Additively Manufactured PA-12 components via a double loop approach [24].

At the core of a random field representation lies the covariance function that models the spatial dependence of the uncertain quantity. When the complete covariance function is known, e.g. by fitting it to an elaborate set of measurement data, discretization of the random field is objective with respect to the available data (see Section 2). However, in order to obtain the complete covariance structure of any random field, data with both a high statistical and spatial resolution are necessary. The argumentation for the former prerequisite is based on the need for an objective estimation of the statistical structure of the non-determinism, whereas the latter is of specific importance to ensure that the spatial effect is accurately quantified. In realistic engineering practice such data are generally not available as the necessary experimental campaign is both highly time consuming and very costly. Therefore, in practice, the auto-covariance properties of a random field are described by a predefined auto-covariance function (also referred to as kernel). When an isotropic random field is considered, these kernels only depend on their correlation length. This length measures the distance between two locations r_i and r_j over which their mutual correlation approaches zero. As such, in the limit case when the correlation length approaches infinity, all realizations of the random field are perfectly correlated, and the field reduces to a random variable. Conversely, when the correlation length tends to zero, an independent random variable is defined for

each location in Ω and the random field represents white noise. Therefore, it can be understood that the correlation length has a significant influence on the realizations of the auto-covariance function, and consequently, the result of the probabilistic calculation. Moreover, it also implicitly determines the number of random variables and corresponding computational cost that is required to accurately determine the random field [25]. Given the major influence of the auto-covariance function on both the spatial aspect of the random field (see e.g., [26] for an in-depth study on the effect of both the functional form of the autocovariance function and corresponding correlation length in a geotechnical context) and its numerical discretization (e.g. following a Karhunen-Loève approach [27]), it is of importance that it is defined with great care [28]. This implies that both the functional form of the auto-covariance, as well as its correlation length need to be selected appropriately. This selection is preferably based on objective data instead of an expert engineering judgement, as lack of an accurately defined covariance structure yields an unrepresentative outcome of the numerical approximation, as e.g. illustrated in [26].

As a remediation for the strict requirements on the data that are necessary to accurately represent quantities in the probabilistic framework, the concept of imprecise probabilities is gaining more and more traction [29]. Following an imprecise probabilistic framework, the analyst acknowledges impreciseness in key attributes of the probabilistic quantities under consideration, rather than assuming a certain crisp value. In practice, this is usually obtained by assigning intervals to the statistical moments of a family of distributions belonging to a predefined credal set [30]. In the context of imprecise random field analysis, Verhaeghe et al. [31] where the first to study the effect of computing with interval-valued correlation lengths in a random field with exponential covariance kernel. Similarly, Dannert et al. [32] recently introduced a p-box framework for the propagation of imprecise random fields with interval-valued correlation length where they select samples from the correlation length interval a priori. Gao et al. [33] also recently proposed an efficient sampling approach to cope with impreciseness in random field analysis to determine bounds on the relia-

bility of structural components under mixtures of stochastic and non-stochastic system inputs.

However, to the best knowledge of the authors, no method exists to effectively and consistently propagate imprecise random fields with parametrized imprecise covariance functions. This paper introduces a generic theoretical framework for describing imprecise random fields extending the current p-box description of imprecise probabilities. Focus on the interval mathematical framework behind interval-valued covariance functions is given to identify and explain the difficulties in propagating imprecise random fields. Furthermore, it proposes an interval approach towards the propagation of imprecise random fields via the Karhunen-Loève (KL) expansion that ensures that a complete basis is generated for the entire range of the correlation length. The paper is structured as follows: Section 2 first recapitulates the most important concepts for random field analysis via the Karhunen-Loève expansion. Then, section 3 introduces a general theoretical framework for describing imprecise random fields, extending the current p-box formalism towards imprecise random fields. This framework is an extension of the work presented by [33] in the sense that it also considers imprecision in the parameters of the random field covariance function. Section 4 first discusses the propagation of imprecise random fields via a double-loop optimization approach and then presents an efficient iterative procedure to first generate a set of complete bases for the propagation of the imprecise random field subjected to an imprecise covariance function in monotonic models. Two case studies on a linear oscillator with random excitation and a car suspension dynamics state-space model are provided in respectively section 5 and 6 to illustrate the developed efficient propagation scheme. These two case studies focus on illustrating the developed efficient propagation scheme for imprecise random field analysis. Finally, section 7 summarizes the conclusions and the outlook for future work.

2. Random field analysis

In a probabilistic context, model parameters $\boldsymbol{x}(\mathbf{r})$ that are subjected to spatial variability are modeled as a random field $x(\mathbf{r}, \theta)$. Such a random field $x(\mathbf{r}, \theta)$ describes a set of correlated random variables $x(\theta)$, assigned to each location $\mathbf{r} \in \Omega$ in the continuous model domain $\Omega \subset \mathbb{R}^d$ with dimension $d \in \mathbb{N}$. Each such a random variable $x(\theta)$ provides a mapping $x : (\Theta, \varsigma, P) \mapsto \mathbb{R}$ with $\theta \in \Theta$ a coordinate in sample space Θ and ς the sigma-algebra. For a given event θ_i, $x(\mathbf{r}, \theta_i)$ is a realization of the random field. A random field is considered Gaussian if the distribution of $(x(\mathbf{r}_1, \theta), x(\mathbf{r}_2, \theta), \ldots, x(\mathbf{r}_n, \theta))$ is jointly Gaussian $\forall \mathbf{r} \in \Omega$. In this case, $x(\mathbf{r}, \theta)$ is completely described by its mean function $\mu_x(\boldsymbol{r}) : \Omega \mapsto \mathbb{R}$ and its auto-covariance function $\boldsymbol{\Gamma}_x(\mathbf{r}, \mathbf{r'}) : \Omega \times \Omega \mapsto \mathbb{R}$. Commonly, (squared) exponential or Matérn covariance functions are applied [26].

In an engineering context, the application of random fields for the modeling of spatial non-deterministic material quantities requires a discretization of $\boldsymbol{x}(\mathbf{r})$ over Ω. Specifically, this means that the continuous random field $x(\mathbf{r}, \theta)$ is represented by a finite set of $M \in \mathbb{N}^+$ correlated random variables $\zeta_i, i = 1, \ldots, M$, as well as a set of deterministic functions that describe the spatial behavior of the field. Usually, such discretization is obtained following a Karhunen-Loève (KL) series expansion [34]. At the core of the method lies a spectral decomposition of a continuous, bounded, symmetric and positive definite auto-covariance function $\boldsymbol{\Gamma}_x(\mathbf{r}, \mathbf{r'}) : \Omega \times \Omega \mapsto \mathbb{R}$ following Mercer's theorem:

$$\boldsymbol{\Gamma}_x(\mathbf{r}, \mathbf{r'}) = \sum_{i=1}^{\infty} \lambda_i \boldsymbol{\psi}_i(\mathbf{r}) \boldsymbol{\psi}_i(\mathbf{r'}) \tag{1}$$

where $\lambda_i \in [0, \infty)$ and $\boldsymbol{\psi}_i(\mathbf{r}) : \Omega \mapsto \mathbb{R}$ are respectively the eigenvalues and eigenfunctions of $\boldsymbol{\Gamma}_x(\mathbf{r}, \mathbf{r'})$. These are in practice obtained by solving the homogeneous Fredholm integral equation of the second kind:

$$\int_{\Omega} \boldsymbol{\Gamma}_x(\mathbf{r}, \mathbf{r}') \boldsymbol{\psi}_i(\mathbf{r}') d\mathbf{r}' = \lambda_i \boldsymbol{\psi}_i(\mathbf{r}). \tag{2}$$

Since $\boldsymbol{\Gamma}_x(\mathbf{r}, \mathbf{r}')$ is bounded, symmetric and positive semi-definite, and furthermore in most practical cases can be assumed positive definite, these eigenvalues

λ_i are non-negative and the eigenfunctions $\boldsymbol{\psi}_i(\mathbf{r})$ satisfy following orthogonality condition:

$$\left\langle \boldsymbol{\psi}_i(\mathbf{r}), \boldsymbol{\psi}_j(\mathbf{r}) \right\rangle = \int_{\Omega} \boldsymbol{\psi}_i(\mathbf{r}) \boldsymbol{\psi}_j(\mathbf{r}) d\mathbf{r} = \delta_{ij} \tag{3}$$

with δ_{ij} the Kronecker delta and $\langle \cdot, \cdot \rangle : \Omega \times \Omega \mapsto \mathbb{R}$ an inner product space. Hence, the eigenfunctions form a complete orthogonal basis on a $\mathcal{L}_2$ space. In this case, the series expansion in eq. (1) is convergent [34]. As such, the random field can be expressed as a series expansion:

$$x(\mathbf{r}, \theta) = \mu_x(\mathbf{r}) + \sigma_x \sum_{i=1}^{\infty} \sqrt{\lambda_i} \boldsymbol{\psi}_i(\mathbf{r}) \xi_i(\theta) \tag{4}$$

with σ_x the standard deviation of the random field (in case $\boldsymbol{\Gamma}_x(\mathbf{r}, \mathbf{r'}) : \Omega \times \Omega \mapsto [0, 1]$) and $\xi_i(\theta), i = 1, \ldots, \infty$ standard uncorrelated random variables, which are determined following:

$$\xi_i(\theta) = \frac{1}{\sqrt{\lambda_i}} \int_{\Omega} \left[x(\mathbf{r}, \theta) - \mu_x(\mathbf{r}) \right] \boldsymbol{\psi}_i(\mathbf{r}) d\mathbf{r} \tag{5}$$

which can be shown to be independent standard normally distributed in the case of a Gaussian random field. In case the field is non-Gaussian, the joint distribution of $\xi_i(\theta)$ is practically very hard to obtain. Therefore, non-Gaussian random fields are typically processed as functions of Gaussian random fields via non-linear mappings on the discretized random field [35, 36, 37].

To limit the computational cost, the series expansion in eq. (4) is usually truncated by retaining only the $Q \in \mathbb{N}$ largest eigenvalues and corresponding eigenfunctions of $\boldsymbol{\Gamma}_x(\mathbf{r}_i, \mathbf{r}_j)$ [38], which yields an optimal series expansion with respect to the global mean squared error [39]. Formally, this is expressed as:

$$\tilde{x}(\mathbf{r}, \theta) = \mu_x(\mathbf{r}) + \sigma_x \sum_{i=1}^{Q} \sqrt{\lambda_i} \boldsymbol{\psi}_i(\mathbf{r}) \xi_i(\theta). \tag{6}$$

A closed form solution for the Fredholm integral equation presented in eq. (2) exists only for very simple domains and Gaussian random fields. Therefore, it is usually approximated via numerical methods such as numerical integration via Nystrom's method or Galerkin projection to find a finite dimensional representation of the basis functions. For a recent overview on numerical

procedures, the reader is referred to [28]. The discretization of a continuous random field $x(\mathbf{r}, \theta)$ into $\tilde{x}(\mathbf{r}, \theta)$ inevitably introduces an approximation error $\epsilon_x(\mathbf{r}, \theta) = x(\mathbf{r}, \theta) - \tilde{x}(\mathbf{r}, \theta)$, which is defined as the distance between the continuous and the discretized random field. Usually, the global mean square error is applied to quantify the error made by the approximation:

$$\bar{\epsilon}_x^2 = \int_{\Omega} E\left[\epsilon_x(\mathbf{r}, \theta)^2\right] d\mathbf{r} \tag{7}$$

with $E[\cdot]$ the expectation operator. Also other error metrics are commonly applied [28].

Usually, an analyst is interested in the response of the structure or system under consideration given the random field description of some model quantities. Let $\mathcal{M}$ be a deterministic numerical model that approximates $\boldsymbol{y} \in \mathbb{R}^d$, the solution of a set of differential equations describing the physics of the considered structure through a set of (usually) real-valued function operators $\boldsymbol{g} = \{g_i \mid i = 1, \ldots, d_s\}$:

$$\mathcal{M}(\boldsymbol{x}) : \boldsymbol{y} = g_i(\boldsymbol{x}), \qquad g_i : \mathbb{R}^k \mapsto \mathbb{R}, i = 1, \ldots, d_s \tag{8}$$

with $\boldsymbol{x} \in \mathcal{F} \subset \mathbb{R}^k$ the vector of model parameters and $\mathcal{F}$ the sub-domain of feasible parameters (e.g., non-negative contact stiffness). Then, statistical properties of $\boldsymbol{y}$ are obtained by generating realizations of $\tilde{\boldsymbol{x}}(\mathbf{r}, \theta_i),\ i = 1, \ldots, N$ over Ω by drawing $N \in \mathbb{N}^+$ samples from the independent standard normal random variables $\xi_i(\theta),\ i = 1, \ldots, Q$ following a Monte Carlo sampling approach. Then, each of these realizations is propagated through the numerical model $\mathcal{M}$:

$$\boldsymbol{y}\left(\mathbf{r}, \theta_i\right) = \mathcal{M}\left(\tilde{\boldsymbol{x}}\left(\mathbf{r}, \theta_i\right)\right) \quad i = 1, \ldots, N. \tag{9}$$

Generally, N should be sufficiently large to allow for an accurate estimation of the joint probability structure of $\boldsymbol{y}(\mathbf{r}, \theta)$. For instance, following a regular Monte Carlo approach, the variance on the estimation of the mean is shown to decrease $\propto 1/\sqrt{N}$. Other, more efficient sampling schemes have been introduced in literature as well [40]. In an intrusive setting, stochastic Galerkin is commonly applied to solve the propagation problem [39].

3. Imprecise random field analysis

In case a Gaussian random field $x(\mathbf{r}, \theta)$ with a parameterized auto-covariance function $\mathbf{\Gamma}_{\boldsymbol{x}}(L)$ with $L \in \mathbb{R}^+$ the correlation length, is considered over the domain Ω, it is fully described by the triplet $(\boldsymbol{\mu}_x, \sigma, L)$. However, in engineering practice, it is often difficult or even intractable to objectively provide a crisp estimate for these quantities, leading to often-subjective estimates to obtain a random field description of the phenomenon under consideration. Especially given the importance of the correlation length on both the numerical and statistical aspects of the random field simulation, as explained in the introduction, such approach is not desirable. This led to the so-called concept of imprecise random fields, which are deeply rooted in the broader concept of imprecise probabilities, and more specifically, the field of probability boxes (p-box). A p-box models a class of probability functions, defined between left and right bounds of their cumulative distribution functions, enriched with constraints on the mean, standard deviation and distribution shape [29]. Specifically, a p-box $[x]$ is defined by the quintuplet $(\overline{F}, \underline{F}, \mu_x^I, \sigma_x^I, \mathcal{F})$ with $\mathcal{F} \subset \mathfrak{F}$ the set of admissible distribution functions belonging the class of probability functions $\mathfrak{F} = \{F \mid F : \mathbb{R} \mapsto [0,1], \forall x, y : x < y \iff F(x) < F(y)\}$. $\overline{F}$ and $\underline{F}$ represent the left and right bounds of the cumulative distribution functions bounding the P-box. As such, a p-box is fully defined by the three following constraints:

$$\underline{F} \leq F \leq \overline{F} \tag{10a}$$

$$\int_{-\infty}^{\infty} x dF(x) \in \mu^I \tag{10b}$$

$$\left(\int_{-\infty}^{\infty} x^2 dF(x)\right) - \left(\int_{-\infty}^{\infty} x dF(x)\right)^2 \in \sigma_x^I. \tag{10c}$$

In the context of a random field $x(\mathbf{r}, \theta)$, given epistemic uncertainty on (some of) its hyper-parameters, the field becomes an imprecise random field $[x](\mathbf{r}, \theta)$. In this case, for completeness, also the set of admissible covariance structures of the random field should be bounded. Hence, an imprecise random field is defined

by the sextuplet $(\overline{F}, \underline{F}, \mu_x^I, \sigma_x^I, \mathcal{F}, \mathcal{C})$, with $\mathcal{C}$ the set of admissible covariance functions. In the specific case of an imprecise random field with a (quadratic) exponential or Matérn covariance kernel, this reduces to $(\overline{F}, \underline{F}, \mu_x^I, \sigma_x^I, \mathcal{F}, L^I)$. The KL expansion of an imprecise random field in this case becomes:

$$[x](\mathbf{r}, \theta) = \mu_x^I(\mathbf{r}) + \sigma_x^I \sum_{i=1}^{\infty} \sqrt{\lambda_i^I} \boldsymbol{\psi}_i^I(\mathbf{r}) \xi_i(\theta) \tag{11}$$

with $\lambda_i^I \in \mathbb{IR}$ interval-valued eigenvalues and $\boldsymbol{\psi}_i^I(\mathbf{r}) : \Omega \mapsto \mathbb{IR}$ interval fields representing the bounds on the corresponding eigenfunctions. It can therefore be understood that an imprecise random field describes a set of correlated P-boxes $[x](\theta)$ for each location $\mathbf{r} \in \Omega$. As such, when considering a single location $\mathbf{r}_i \in \Omega$ bounds for the cumulative distribution are locally given. Similarly, for a given θ_i, also realizations $[x](\mathbf{r}, \theta_i)$ are generated. The main difference with the realizations of a regular random field is that in case θ is fixed, the realizations become interval field valued:

$$[x](\mathbf{r}, \theta_i) = \mu_x^I(\mathbf{r}) + \sigma_x^I \sum_{i=1}^{\infty} \sqrt{\lambda_i^I} \boldsymbol{\psi}_i^I(\mathbf{r}) \xi_i(\theta_i). \tag{12}$$

Indeed, since epistemic uncertainty is present in the definition of μ_x, σ_x and L, a full admissible set of realizations that are consistent with these intervals is provided. It should be noted that, in case $\mathcal{F}$ extends towards more than Gaussian random fields, the same considerations concerning the correlation and dependence in ξ_i as made for regular random fields have to be made. Note that for practical purposes, also this series expansion should be truncated after Q terms.

However, some fundamental issues regarding the propagation exist. Consider a covariance function $\boldsymbol{\Gamma}_x$; when its governing parameters (e.g., the correlation length) become interval valued, the function itself becomes interval valued as well. Assume that this function is discretized over a $N \times N$ rectangular grid, as is common in for instance Finite Element computations. In that case, a symmetric, bounded, positive semi-definite interval covariance-matrix $\boldsymbol{\Gamma}^{\boldsymbol{I}} \in \mathbb{IR}^{N \times N}$ is obtained. Following the work in [41], it can be shown that the outer approx-

imation of the eigenvalues of $\mathbf{\Gamma^I}$ is given by:

$$\lambda_i \left(\mathbf{\Gamma}_c - S_i^T \mathbf{\Gamma}_\Delta S_i\right) \leq \lambda_i(\mathbf{\Gamma^I}) \leq \lambda_i \left(\mathbf{\Gamma}_c + S_i^T \mathbf{\Gamma}_\Delta S_i\right) \tag{13}$$

with $i = 1, \ldots, N$, $\mathbf{\Gamma}_c$ and $\mathbf{\Gamma}_\Delta$ respectively the midpoint and radius of the interval covariance matrix $\mathbf{\Gamma^I}$ and $S_i = \text{diag}(\text{sgn}(\boldsymbol{\psi}_i(\mathbf{r})))$. The notation $\lambda_i(\bullet)$ infers the process of computing the i^{th} eigenvalue of the matrix $\bullet$. This theorem holds if S_i is constant over the parameter interval [42]. In general, the bounds for $\boldsymbol{\psi}_i(\mathbf{r})$ do not correspond to the vertices of λ_i^I, and hence, generally they need to be determined following an optimization approach where $\boldsymbol{\psi}_i(\mathbf{r})$ are minimized and maximized with respect to λ^I and while keeping all other $\boldsymbol{\psi}_i(\mathbf{r})$ equal to unity [43]. The bounds for the corresponding eigenvectors $\boldsymbol{\psi}_i(\mathbf{r})$ can in that case be expressed as [42, 44]:

$$\begin{bmatrix} \lambda_i(\mathbf{\Gamma}^I)I - S_i^T \mathbf{\Gamma}_c S_i & -\mathbf{\Gamma}_\Delta \\ S_i^T \mathbf{\Gamma}_c S_i & -\mathbf{\Gamma}_\Delta - \lambda_i(\mathbf{\Gamma}^I)I \end{bmatrix} |\boldsymbol{\psi}_i(\mathbf{r})| \leq 0 \tag{14}$$

with $\lambda_i(\mathbf{\Gamma}^I) \in \lambda_i^I(\mathbf{\Gamma}^I)$. However, following this approach does not guarantee that the corresponding sets of generated basis functions form a set of complete orthogonal bases for $\mathcal{L}_2$. This is a direct result of the by-definition independence between intervals. Indeed, since depicting the bounds on the eigenfunctions as interval vectors automatically encloses all possible spatial realizations of those vectors in between the interval bounds, the orthogonality criterion described in eq. (3) does not longer hold. Hence, a direct interval-arithmetical solution using classical interval arithmetic cannot provide a feasible solution to this problem. The application of interval field formulations or affine arithmetical approaches [45, 46] to bound the spatial realizations could be a solution [12], but this falls outside the scope of this paper.

As a practical example, consider for instance an exponential covariance kernel on a 1D domain $\Omega = [-a, a] \subset \mathbb{R}$. In that case, analytical solutions for the

eigenfunctions and eigenvalues exist and are equal to:

$$\boldsymbol{\psi}_i(\mathbf{r}) = \frac{\cos(\omega_n \mathbf{r})}{\sqrt{a + \frac{\sin(2\omega_n a)}{2\omega_n}}}, \quad \lambda = \frac{2/L}{\omega_n^2 + (1/L)^2}, \quad \text{for } n = \text{even} \tag{15a}$$

$$\boldsymbol{\psi}_i(\mathbf{r}) = \frac{\sin(\omega_n \mathbf{r})}{\sqrt{a - \frac{\sin(2\omega_n a)}{2\omega_n}}}, \quad \lambda = \frac{2/L}{\omega_n^2 + (1/L)^2}, \quad \text{for } n = \text{odd} \tag{15b}$$

with ω_n the natural pulsations of the eigenfunctions, obtained by imposing boundary conditions on the differential equation that corresponds to solving eq. (2) [39]. Note that, since the correlation length is interval-valued, that an interval of natural pulsations is obtained, and hence, the eigenvalues λ also become interval-valued. Furthermore, both the pulsation and the magnitude of the eigenfunctions become interval-valued as well, and hence, they become interval fields. In this case $\boldsymbol{\psi}_i^I(\mathbf{r})$ and λ^I are given as:

$$\boldsymbol{\psi}_i^I(\mathbf{r}) = \frac{\cos(\omega_n^I \mathbf{r})}{\sqrt{a + \frac{\sin(2\omega_n^I a)}{2\omega_n^I}}}, \quad \lambda^I = \frac{2/L^I}{(\omega_n^I)^2 + (1/L^I)^2}, \quad \text{for } n = \text{even} \tag{16a}$$

$$\boldsymbol{\psi}_i^I(\mathbf{r}) = \frac{\sin(\omega_n^I \mathbf{r})}{\sqrt{a - \frac{\sin(2\omega_n^I a)}{2\omega_n^I}}}, \quad \lambda^I = \frac{2/L^I}{(\omega_n^I)^2 + (1/L^I)^2}, \quad \text{for } n = \text{odd}. \tag{16b}$$

Since all $\boldsymbol{\psi}_i^I(\mathbf{r})$ become interval field valued, their orthogonality is no longer guaranteed as this should hold between all combinations of possible realizations of the interval-field valued eigenfunctions. These equations illustrate as well that the eigenvalues and eigenfunctions of a covariance kernel are not a monotonic function of the correlation length, complicating the propagation of the interval on the correlation length towards the exact bounds of the function [3]. This is further illustrated in figures 1 and 2, which show the analytic solution in terms of eigenvalues and eigenfunctions for a 1-dimensional exponential covariance kernel for various values of the correlation length. As can be noted from figure 1, not all eigenvalues of the exponential covariance kernel are a monotonic function of L. Furthermore, some of the eigenfunctions are positively dependent, whereas others are negatively dependent. From figure 2, it is clear that both the amplitude and the pulsation as well as the phasing of the eigenfunctions are a function of L, as predicted by the analytical solutions.

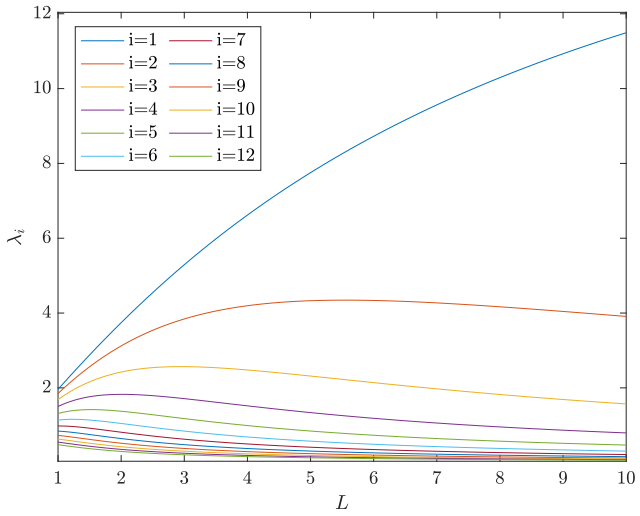

Figure 1: 12 first eigenvalues of the exponential covariance kernel as a function of L. As can be seen, there is not always a monotonic relationship.

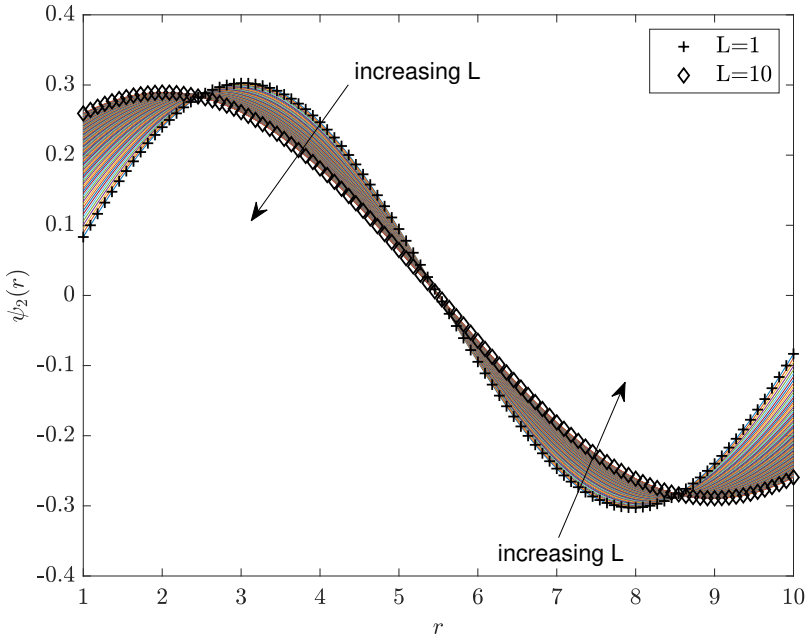

Figure 2: 100 realizations of $\boldsymbol{\psi}_2$ of an exponential covariance kernel between $L = 1$ and $L = 10$, showing that both the phase and amplitude of the eigenfunction are affected.

4. Propagation of imprecise random fields

In this paper, we consider only the case of isotropic imprecise random fields where the appropriate type of covariance kernel and probability density function are known a priori. First, a very general procedure to propagate these fields is shown and its drawbacks discussed. Then, an efficient approach is introduced to propagate these imprecise random fields in case the relationship between the field realizations and the corresponding output parameter is strictly monotonic.

4.1. General propagation

For imprecise random fields, the propagation boils down to the propagation of random field realizations, subjected to the interval-valued uncertainty that is present in the hyper-parameters $\boldsymbol{\mu}_x$, $\boldsymbol{\sigma}_x$ and L, instead of having to consider the full sextuplet $(\overline{F}, \underline{F}, \mu_x^I, \sigma_x^I, \mathcal{F}, \mathcal{C})$. From eq. (6), it is clear that imposing an interval on both $\boldsymbol{\mu}_x$, $\boldsymbol{\sigma}_x$ has a pure monotonous effect on the realizations, hence their propagation can be performed via a vertex approach in case $\mathcal{M}$ is monotonous too [47]. However, as explained in Section 3, the effect of L on the eigenfunctions and eigenvalues of $\boldsymbol{\Gamma}_x$ is not monotonous, and hence, as simple vertex analysis is not conservative in this case. Also an interval-arithmetical approach is not feasible since the bounds on the eigenvectors do not necessarily correspond to the bounds on the eigenvalues of $\boldsymbol{\Gamma}_x$. Furthermore, there exists no guarantee that the sets of bounds on the eigenvectors and their realizations form a complete orthogonal basis, and hence, they are not suitable for use in the KL series expansion. Therefore, we propose to follow an iterative procedure based on global optimization. In a first step, the order of the series expansion is determined, given L^I. Under the assumption that $\boldsymbol{\sigma}^I$ is homogeneous over Ω, the truncation order is determined as the maximum value of Q that is necessary to satisfy following inequality:

$$1 - \frac{1}{|\Omega|} \frac{1}{(\boldsymbol{\sigma}^I)^2} \sum_{i=1}^{Q} \lambda_i(L^I) \leq \epsilon^* \tag{17}$$

with $|\Omega|$ the length, area or volume of the domain depending on the amount of spatial dimensions. This Q value is then subsequently used for all realizations of $L \in L^I$

Consider a general non-monotonic model $\mathcal{M}$ where the bounds of the model's responses not necessarily correspond with the bounds of the hyper-parameter set $\mathcal{H} = (\mu_x, \sigma_x, L)$, or even the bounds on the eigenfunctions of the imprecise random field. The main idea is to apply a global optimization scheme to determine those values $\mathcal{H}^*$ that yield extreme values in a (stochastic) response of the model $\boldsymbol{y}$:

$$\underline{\mathcal{H}} = \underset{\mathcal{M}(\boldsymbol{x}(\mathcal{H}))}{\arg\min}\, y_i, \qquad \text{s.t. } \mu_x \in \mu_x^I, \sigma_x \in \sigma_x^I, L \in L^I \tag{18a}$$

$$\overline{\mathcal{H}} = \underset{\mathcal{M}(\boldsymbol{x}(\mathcal{H}))}{\arg\max}\, y_i, \qquad \text{s.t. } \mu_x \in \mu_x^I, \sigma_x \in \sigma_x^I, L \in L^I \tag{18b}$$

where y can be any sort of (stochastic) quantity depending on the application where the imprecise random field is considered. For instance, it can be the expected value or variance of a response of the system, or even the probability of failure of a structure.

As such, an imprecise random field is propagated following a nested approach where the interval analysis constitutes the outer loop for the propagation of the epistemic uncertainty, whereas the inner loop is concerned with stochastic propagation of the random field corresponding to a realization of $\mathcal{H} \in [\underline{\mathcal{H}}, \overline{\mathcal{H}}]$. For each step during the iterative optimization procedure, a certain set $\mathcal{H}$ is generated for which a full random field simulation needs to be performed to assess the corresponding response y. For instance, considering an interval Monte Carlo [48] implementation for imprecise random fields, while assessing the bounds on the probability of failure of a structure, the optimization problem would be:

$$\underline{P}_f = \frac{1}{N} \sum_{i=1}^{N} I\left[\min(G(\boldsymbol{x}(\mathcal{H}, \theta)) \leq 0)\right] \tag{19a}$$

$$\overline{P}_f = \frac{1}{N} \sum_{i=1}^{N} I\left[\max(G(\boldsymbol{x}(\mathcal{H}, \theta)) \leq 0)\right] \tag{19b}$$

with I the indicator function and G the limit state surface of the problem at

hand.

Since in general, the optimization problem corresponding to the min and max operations is not convex, gradient based optimizers are very susceptible to make under-conservative estimates due to local optima. Therefore, global (meta-heuristic) optimization algorithms should be applied, which may prove to be computationally intractable when real finite element models are considered. As such, following this approach, it is hard to make an a priori estimate of the computational cost as it is highly dependent on the topology of $\mathcal{M}$. Furthermore, in most cases, such approach is intractable without resorting to high-performance computing facilities or surrogate models such as polynomial chaos expansions [49]. Alternatively, the recent introduced framework of Non-instrusive Stochastic Simulation (NISS) can be applied in this context [30].

4.2. An efficient approach for monotonic problems

In some cases, the responses y of $\mathcal{M}$ do have a monotonic relation with respect to the basis functions of the imprecise random field. In those cases, the optimization problem introduced in eq. (18) can be simplified greatly, since only the bounds on the basis functions need to be considered, rather than the full epistemic uncertainty that is present in the definition of the imprecise random field. This section presents such an efficient approach for the specific application of the solution of transient dynamic problems, where the loading of the system, structure or component is modeled as an imprecise random field.

Consider the case of a transient dynamic problem, which is governed by the dynamic equation:

$$M\ddot{X}(t) + C\dot{X}(t) + KX(t) = F(t) \tag{20}$$

with $\ddot{\bullet}$ and $\dot{\bullet}$ representing respectively the second and first time derivative of $\bullet$ and $M \in \mathbb{R}^{n_{dof} \times n_{dof}}, C \in \mathbb{R}^{n_{dof} \times n_{dof}}$ and $K \in \mathbb{R}^{n_{dof} \times n_{dof}}$ respectively the mass, damping and stiffness matrices of the system under consideration. $X \in \mathbb{R}^{n_{dof}}$ is the solution of this ODE and represents a displacement vector. In case

the system is discretized by a finite element model, the terms in X represent the nodal displacements.

Let $H(t)$ denote the impulse response function of the system at a certain time instant τ. When the force excitation $F(t)$ is discretized into n_t time steps Δt, the response $x(t_j)$ at a time instant $t_j,\ j = 1, \ldots, n_t$ is given by:

$$X(t_j) = \sum_{i=1}^{j} F(t_i) H(t_j - t_i) \Delta t. \tag{21}$$

In the limit case where $\lim_{\Delta t \to 0}$, the problem reduces to the solution of the following convolution integral:

$$X(t) = \int_0^t F(\tau) H(t - \tau) d\tau. \tag{22}$$

Hence, in case $H(t - \tau)$ is a monotonic function of t, $X(t)$ is a monotonic function as well with respect to $F(t)$. Now, considering $F(t)$ as being governed by an imprecise random field, the propagation of the uncertainty can be greatly simplified with respect to the general case explained in eq. (18). Indeed, in this case it is sufficient to propagate only those values in $\mathcal{H}$ that bound the eigenfunctions $\sqrt{\lambda_i}\psi_i(\mathbf{r})$ of the imprecise random field.

Let $\mathcal{G}(\Omega, L) : \Omega \times L \mapsto \{\boldsymbol{\lambda}, \boldsymbol{\psi}(\mathbf{r})\}$ denote the process of solving eq. (2) for Q eigenpairs of $\mathbf{\Gamma}_x$ given a crisp value for L (e.g., following Galerkin or Nyström procedures), The main idea is to apply a global optimization scheme to determine those values for L that yield extreme values in $\sqrt{\lambda_i}\boldsymbol{\psi}_i(\mathbf{r})$:

$$\underline{L}_i^* = \arg\min_{\mathcal{G}(L)} ||\sqrt{\lambda_i}\psi_i(\mathbf{r})||_2, \qquad \text{s.t. } L \in L^I \tag{23a}$$

$$\overline{L}_i^* = \arg\max_{\mathcal{G}(L)} ||\sqrt{\lambda_i}\psi_i(\mathbf{r})||_2, \qquad \text{s.t. } L \in L^I \tag{23b}$$

with $i = 1, \ldots, Q$. The underlying idea to look for those L that correspond to extrema in the $\mathcal{L}_2$ norm of the basis function in each mode of the random field is that as such, a complete bounding set is obtained. Furthermore, due to the differentiability of the $\mathcal{L}_2$ norm, this is a smooth, convex, non-linear optimization problem in limited dimension. Therefore, any sequential quadratic

programming approach can be followed to obtain the bounds without excessive computational overhead. Note that the problem is not necessarily convex. As such, it is advised to try different randomized initial estimates.

The maximally $2m$ solutions are then concatenated in a single vertex set $\mathcal{L}$:

$$\mathcal{L} = \left\{ \underline{L}_1^*, \overline{L}_1^*, \underline{L}_2^*, \overline{L}_2^*, \ldots \underline{L}_Q^*, \overline{L}_Q^*, \right\} \tag{24}$$

and the eigen pairs $\boldsymbol{\lambda}, \boldsymbol{\psi}(\mathbf{r})$ are computed using (2) for each of these $L \in \mathcal{L}$. In this way, a set of complete orthogonal bases with corresponding scale factors is obtained that bound the possible variation in the imprecise random field basis, given the interval uncertainty on the correlation length. It should be noted that due to the smoothness of the decay of the eigenvalues of $\boldsymbol{\Gamma}$, the cardinality $\mathfrak{C}(\mathcal{L})$ of $\mathcal{L}$ will be considerably smaller than $2Q$ in practice for commonly applied covariance functions, as will also be clear from the examples in sections 5 and 6.

Finally, for the propagation of the imprecise random field, a consistent admissible set for the interval-valued hyper-parameters should be generated. Let $\mathcal{L}$ denote the admissible set of correlation lengths that are necessary to bound the basis functions of the random field, and let $\mathcal{T} = \left\{ \mu_x^I, \sigma_x^I \right\}$ denote the set of interval-valued hyper-parameters of the distribution function of the imprecise random field. In case a vertex approach is applied for the propagation, $\binom{\mathcal{L} \cup \mathcal{T}}{\mathfrak{C}(\mu_x, \sigma_x, L)}$ realizations of the epistemic uncertainty are needed. It should be noted that in this way, each realization of the admissible set yields a complete basis on $\mathcal{L}_2$ for the construction of realizations of the random field, and as such, the convergence of the KL expansion is still guaranteed. Then, for each of these vertex combinations of the admissible set $\mathcal{L} \cup \mathcal{T}$ of hyper-parameters, a full Monte Carlo propagation consisting of N deterministic model runs of the corresponding random field is performed.

It should be noted that this method is equally applicable to both Gaussian and non-Gaussian random fields. Evidently, in case of non-Gaussian random fields, more computational work is needed to determine $\xi_i(\theta)$ in eq. (6) (e.g.,

following the iterative approach presented in [37]), but this has no effect on the spatial correlation of the field. It is self-evident that the computational cost in this case will increase, as the iterative procedure to determine $\xi_i(\theta)$ needs to be combined with the optimization problem in eq. (23). A more elaborate framework to perform this scheme falls outside the scope of this paper.

4.3. Eigenfunction cross-over

There exists no guarantee that the eigenfunctions $\boldsymbol{\psi}_i$ of $\boldsymbol{\Gamma}_x$ maintain the same ordering for all values of L during the optimization procedure presented in eq. (23). Evidently, this poses large problems for the used optimization algorithms, as in this way discontinuities are introduced during optimization. Therefore, it is proposed to use Modal Assurance Criterion (MAC)-based mode tracking, as is commonly applied in the structural dynamics community to track structural eigenmodes corresponding to resonance frequencies [50].

MAC-based mode tracking, as the name suggests, is inherently based on the Modal Assurance Criterion (MAC) for comparing the similarity of two mode shapes vectors. The MAC provides a measure for the degree to which two mode shape vectors $\boldsymbol{\phi}_i$ and $\boldsymbol{\phi}_j$ are similar. It is defined as:

$$MAC(\boldsymbol{\psi}_i, \boldsymbol{\psi}_j) = \frac{(\boldsymbol{\psi}_i^T \boldsymbol{W} \boldsymbol{\psi}_j)^2}{(\boldsymbol{\psi}_i^T \boldsymbol{W} \boldsymbol{\psi}_i)(\boldsymbol{\psi}_j^T \boldsymbol{W} \boldsymbol{\psi}_j)} \tag{25}$$

with $\boldsymbol{W}$ a weighting matrix, which can safely be chosen as unity in the case of simulated eigenfunctions of a random field. When the considered eigenfunctions are closely related, the MAC value tends to one. When different eigenfunctions of the same random field are considered, the MAC value is zero, as they are orthogonal by definition (see eq. (3)). Values between zero and one are obtained when either the same eigenfunction is considered between different random fields, for instance when varying the correlation length in between the predefined bounds. Using the properties of the eigenfunctions, as discussed in Section 2, eq. (26) can be reduced to:

$$MAC(\boldsymbol{\psi}_i, \boldsymbol{\psi}_j) = (\boldsymbol{\psi}_i^T \boldsymbol{\psi}_j)^2. \tag{26}$$

A first intuitive approach to reorder the eigenfunctions in this solution is to sequentially pair the eigenfunctions with the highest MAC value to the reference eigenfunctions, based on the MAC matrix. This however is generally not the best solution, as the matching of the eigenfunctions corresponding to the lowest eigenvalues can become very poor. The tracking of the eigenfunctions of the random fields is therefore performed as follows:

1. Solve eq. (2) for a predefined correlation length $\hat{L} \notin L^I$ in order to obtain a reference configuration $\hat{\boldsymbol{\lambda}}, \hat{\boldsymbol{\psi}}$. Taking $\hat{L} \notin L^I$ prevents ambiguous mixed eigenfunctions that possibly complicate the eigenfunction matching
2. During the solution of eq. (23), perform following iteration:
   (a) sort MAC values for each combination of ψ_i, ψ_j in decreasing order for each ψ_i and construct index set $\mathcal{I}_o$;
   (b) compute $\delta_i = MAC(\psi_i, \psi_{\mathcal{I}_o(1)}) - MAC(\psi_i, \psi_{\mathcal{I}_o(2)})$, with $\delta \in [0, 1]$, which is a measure for how clear an eigenfunction ψ_i is the best fit for the corresponding reference eigenfunction $\hat{\psi}_i$;
   (c) link ψ_i satisfying $\max_i(\delta_i)$ to ψ_j satisfying $\max_j MAC(\psi_i, \psi_j)$;
   (d) remove ψ_i and ψ_j from set of eigenfunctions to be reordered.

A more elaborate explanation of this algorithm, as well as an example of its application is given by [51].

5. Case study 1: Linear oscillator with random excitation

5.1. Case presentation

This case study concerns a simple mass-spring-damper system, subjected to a random excitation, as described by eq. (20). The mass m, damper c and spring k are modeled as being deterministic, and their values are respectively taken to be $m = 1kg$, $c = 2N \cdot s/m$ and $k = 10N/m$. The initial conditions are set as $x(0) = 0\ m$ and $\dot{x} = 0\ m/s$. The system is solved for $x(t)$ for $t \in [0, 20]\ s$. The excitation of the system is modeled as an imprecise Gaussian random field with $\mu_F^I = [0.5, 1.5]\ N$, $(\sigma_F^I)^2 = [\sqrt{2}, 2]\ N^2$ and $L^I = [2, 7.5]\ s$, over a 1-dimensional domain $\Omega_F = [0, 20]\ s$. Four types of covariance functions are considered:

- exponential covariance:

$$\Gamma_F = \exp(\frac{-|t_2 - t_1|}{L}) \tag{27}$$

with t_i a time instance during the excitation.

- modified exponential covariance [52]:

$$\Gamma_F = \exp\left(-\frac{|t_2 - t_1|}{L}\right)\left(1 + \frac{|t_2 - t_1|}{L}\right) \tag{28}$$

- squared exponential covariance:

$$\Gamma_F = \exp(-\frac{(t_2 - t_1)^2}{L^2}) \tag{29}$$

- Whittle-Matérn covariance:

$$\Gamma_F = \frac{1}{G(\nu)2^{\nu-1}}\left(\sqrt{2\nu}d\right)^{\nu} K_\nu\left(\sqrt{2\nu}d\right) \tag{30}$$

  with $G(\bullet)$ the gamma function, K_ν the modified Bessel function of the second kind, $d = (t_2 - t_1)$ the distance and ν a non-negative parameter of the covariance. In this case, it is chosen as $\nu = 1.5$.

5.2. Discretization of the imprecise random field

For each of the considered covariance functions, the effect of the interval on the correlation length is studied. Hereto, the domain $\Omega_F \subset \mathbb{R}$ is discretized into 100 equally spaced time intervals $\Omega_{F,e}$ and F is considered constant over each $\Omega_{F,e}$. The interval eigenvalue problem, as presented in eq. (2), is solved by means of a Galerkin procedure assuming a single set of basis functions for Ω_F retaining the 9 first terms of the expansion.

Figure 3 illustrates the result of the optimization problem presented in eq. (23). As can be noted, the procedure is capable of identifying those correlation lengths in L^I that produce a bound on $\sqrt{\lambda_i}\boldsymbol{\psi}_i(\mathbf{r})$ that hold for the entire domain Ω. Since a set of $\sqrt{\lambda_i}\boldsymbol{\psi}_i(\mathbf{r})$ is used to bound the domain, rather than a single set of bounds, it is ensured that the basis over Ω is still orthogonal, and hence, the KL expansion retains its properties as explained in Section 2. Note that only

the four first $\sqrt{\lambda_i}\boldsymbol{\psi}_i(\mathbf{r})$ are shown for the sake of clarity. Therefore, it might not be entirely clear that indeed each of the realizations is necessary to bound all $\sqrt{\lambda_i}\boldsymbol{\psi}_i(\mathbf{r})$ for each $t \in \Omega_t$.

Furthermore, the cardinality of $\mathcal{L}$ depends for the same correlation length interval on the covariance function under consideration. For the exponential, modified exponential, squared exponential and Whittle-Matérn covariance functions with $L^I = [2, 7.5]$ s is respectively 6, 4, 7 and 10. This is directly linked to the smoothness of the realizations of the underlying random field at the given set of correlation lengths.

The effect of the width of the correlation length on the cardinality of $\mathcal{L}$ is also illustrated in figure 4. In this figure, the upper bound $\overline{L}$ is kept constant at 7.5 s, while the lower bound is gradually increased as

$$\underline{L} = [2, 2.55, 3.11, 3.66, 4.22, 4.77, 5.33, 5.88, 6.44, 7, 7.2, 7.4, 7.45] \ s$$

in order to decrease the width of the interval. As this figure shows, in case L^I is wider, more terms are necessary to capture the non-monotonicity in the KL basis. This is in fact logic since the interval on the correlation length both affects the amplitude as the periodicity of the basis functions, as is illustrated for the exponential kernel in figure 2, as well in figure 3 for all considered kernel functions. Since the necessary number of deterministic model evaluations scales exponentially with the cardinality of this set, this has large implications on the computational cost of propagating the imprecise random field. Furthermore, it may be noticed that the problem does not become monotonic, even when very thin intervals on the correlation length are considered.

5.3. Propagation of the imprecise random field

As a final step in this illustrative example, the imprecise random field that is discretized using the methodology presented in this paper is applied as a random excitation to the linear oscillator. As stated in Section 4, the monotonicity of the responses of a system depend on the quantity under consideration. This condition is met for this specific model.

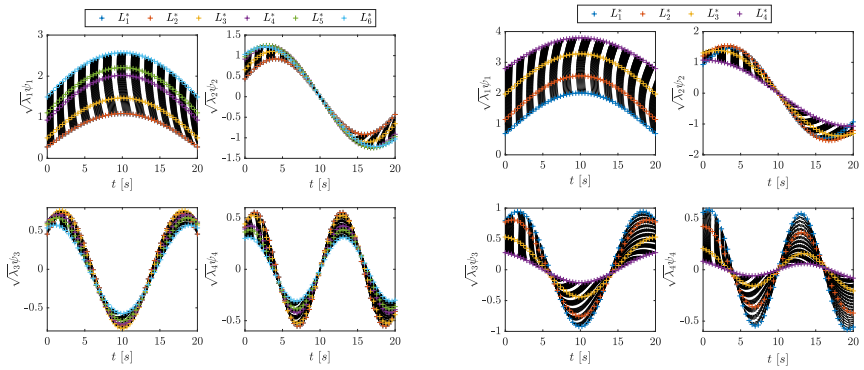

(a) Exponential

(b) Modified exponential

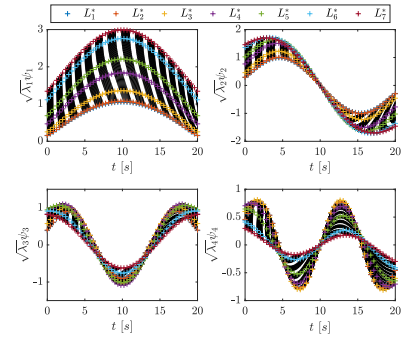

(c) Squared exponential

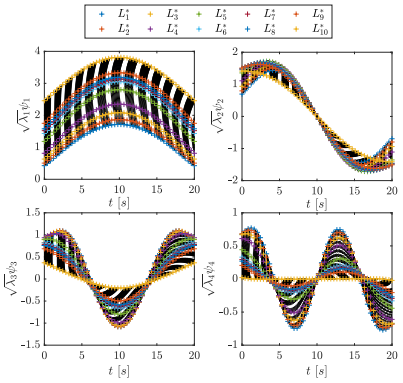

(d) Whittle-Matérn

Figure 3: Bounds on $\sqrt{\lambda_i}\boldsymbol{\psi}_i(\mathbf{r})$, obtained by solving the optimization problem introduced in eq. (23) in combination with Galerkin on four covariance functions on a 1-dimensional domain $\Omega_F = [0, 20]$ s discretized in 20 elements.

As a first example, consider the failure probability of this system as the probability that the displacement of the mass exceeds a certain threshold x_t within the considered time. For the stochastic propagation, a Monte Carlo simulation containing 5000 samples was used at each vertex of $\mathcal{H}$. The bounds on the probability of failure are computed using the bounds on the basis functions, as computed in the previous sections, and are compared with the bounds on the probability of failure, computed using 150 samples of a Sobol sequence that was generated in between the bounds of $\mathcal{H}$, resulting in a total of $750,0000$ ODE

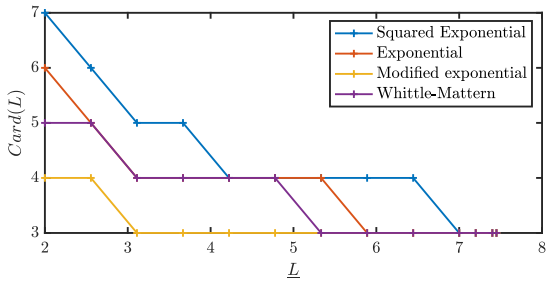

Figure 4: Cardinality of the admissible set of correlation lengths as a function of the width of the interval on L^I.

solves. The same seed was used for the stochastic propagation of both sets. The latter set is propagated to assert that indeed in this case the bounds on the basis functions provide the analyst with the bounds on the failure probability.

Figure 5 shows the bounds on the probability of failure for different values of x_t. These bounds are computed by assessing the probability of failure given each random time signal corresponding to a vertex of $\mathcal{H}$. As can be noted, propagating the bounds on the basis functions indeed bounds the probability of failure of the linear oscillator at greatly reduced cost compared to propagating the Sobol set. Indeed, in this case, only 60000 calls to the deterministic ODE solver are necessary, as compared to $750,000$ for the propagation of the Sobol set. Note that the lower bounds on the probability of failure are missing for high threshold values. This is due to the rather limited set of Monte Carlo samples.

Furthermore, also in case the analyst is interested in the cumulative density function of the response of the oscillator on a given time instant, the propagation of the parameters that yield the bounds of the basis functions bounds the epistemic uncertainty of this response for this case study. This is illustrated in figure 6. This figure shows p-boxes on displacement values of the oscillator, evaluated at $t = 1\ s$, $t = 4\ s$ and $t = 15\ s$, predicted by propagating the bounds on the basis functions and fitting empirical cumulative density functions to each of the random field propagations corresponding to a vertex of the hyper-cubic uncertain hyper-parameter set. Also, for each realization of this

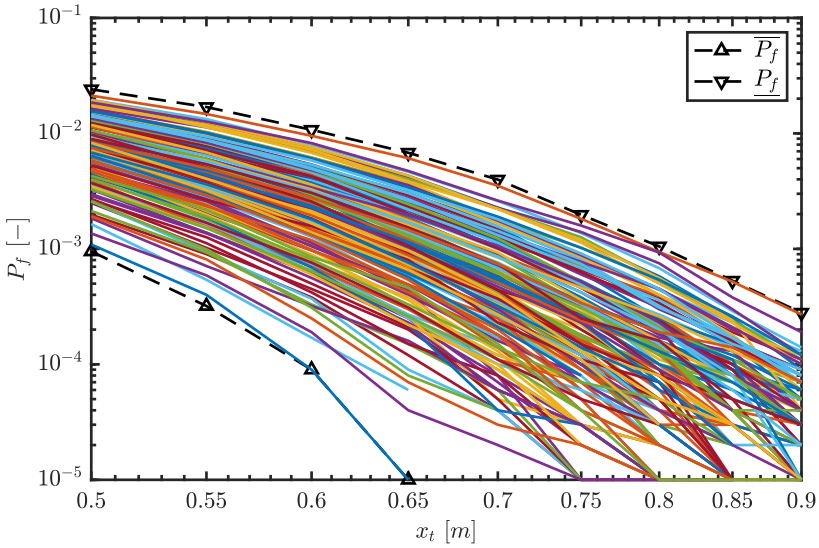

Figure 5: Bounds on the probability of failure in case different threshold values are used.

hyper-parameter set, obtained by the Sobol sequence, an empirical cumulative density function is fitted. As can be seen, the p-box that is obtained by propagating the parameters that bound the basis functions of the imprecise random field, also bounds the cumulative density functions in between those bounds. This is a direct result from the fact that the model is a pure linear oscillator subjected to a random excitation, and hence, is monotonic with respect to the imprecise random field on the load. As such, the conditions for applying the efficient propagation methodology are met.

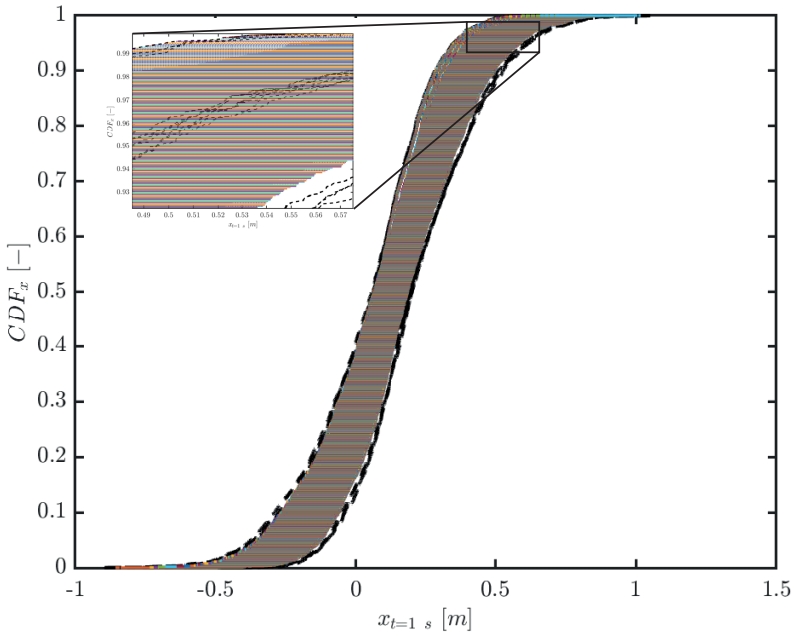

Figure 6: Bounds on the cumulative distribution of displacement values of the oscillator, evaluated at $t = 1\ s$, predicted by propagating the bounds on the basis functions, as well as by propagating the Sobol set on the hyper-parameters.

6. Case study 2: Vehicle suspension comfort estimation

The second case study is concerned with assessing the bounds on the comfort of a vehicle suspension, given an imprecise random field description of the road profile. Hereto, a quarter-car model is applied to model the car dynamics. Also this system can be regarded as a linear transient dynamic system of the form shown in eq. (20), and hence, the application of the method introduced in Section 4 will yield the exact bounds on the responses of the model. For this specific case, a state-space model is employed:

$$\frac{d}{dt}\begin{bmatrix} x_{us}-x_0 \\ \dot{x}_{us} \\ x_s - x_{us} \\ \dot{x}_s \end{bmatrix} = A \begin{bmatrix} x_{us}-x_0 \\ \dot{x}_{us} \\ x_s - x_{us} \\ \dot{x}_s \end{bmatrix} + \begin{bmatrix} -1 \\ \frac{4c_t}{m_{us}} \\ 0 \\ 0 \end{bmatrix} \dot{x}_0 \tag{31}$$

with x_{us} the displacement of the unsprung mass, x_s the displacement of the sprung mass, $\dot{\bullet}$ the time derivative of $\bullet$, m_{us} and m_s the unsprung and sprung mass of a quarter of the car, c_s and c_t respectively the damping coefficients of the suspension and tire, k_s and k_t respectively the stiffness coefficients of the suspension and tire and the matrix A equal to:

$$A = \begin{bmatrix} 0 & 1 & 0 & 0 \\ \frac{-4k_t}{m_{us}} & \frac{-4(c_s+c_t)}{m_{us}} & \frac{4k_s}{m_{us}} & \frac{4c_s}{m_{us}} \\ 0 & -1 & 0 & 1 \\ 0 & \frac{4c_s}{m_s} & \frac{-4k_s}{m_s} & \frac{-4c_s}{m_s} \end{bmatrix}. \tag{32}$$

The system is excited at the basis, with x_0 modeling the vertical displacement of the tire. The complete road profile is denoted $x_0(t)$. Four state variables are considered, being respectively the tire deflection; the unsprung mass velocity; the suspension stroke, and sprung mass velocity. Typically, in the context of assessing the comfort of a car, two parameters are of interest: the suspension stroke (i.e., the relative displacement of the car body with respect to the unsprung mass) and the acceleration of the sprung mass (car body).

In this example, the suspension of the car is tuned for performance. The parameters of the state-space model are listed in table 1. The dynamics of the

car are simulated over a distance of 100 m, when the car is traveling at a speed of 10 m/s. The one-dimensional spatial domain is discretized into 200 equidistant points and the time domain is discretized into time intervals of 0.005 s

Table 1: Parameters of the quarter car state-space model

Parameter	Value
m_s	325 kg
m_{us}	65 kg
$c_s + c_t$	1898 N.s/m
k_t	2325 N/m
k_s	505 N/m

The uncertain road profile is modeled as a zero-mean imprecise Gaussian random field with exponential covariance kernel. Imprecision is present in the variance σ^2 of the field, as well as in the correlation length L of the covariance kernel. The former corresponds in this case to to the height of road roughness values, whereas the latter corresponds to their spatial frequency. Specifically, the intervals on the variance and correlation length are respectively set as $(\sqrt{\sigma^I})^2 = [0.0015; 0.003]$ m and $L^I = [2; 15]$ m.

A solution to the optimization problem introduced in eq. (23) indicates that a set $\mathcal{L}$ with cardinality of 16 is necessary to capture all spatial variation. This is a direct result from the comparably large interval on the correlation length (see also figure 4 of case study 1). As such, 32 vertex combinations are needed to propagate the epistemic uncertainty in the imprecise random field. The stochastic propagation is performed by means of Monte Carlo simulation with 1000 samples. The results of this propagation are compared to a simulation where the epistemic uncertainty is propagated using a Sobol set consisting of 500 samples in between the intervals on σ^I and L^I.

Figure 7 illustrates those stochastic realizations of the Sobol set in the hyper-parameters that yield an extremum in the acceleration profile of the sprung mass

during the time interval $[0, 2]$ s, as well as the extreme bounds $[\underline{a}(t); \overline{a}(t)]$ that are predicted by taking:

$$\underline{a}(t_i) = \min a(t_i \mid \mathcal{L} \cup \mathcal{T}, \theta) \qquad \forall t_i \in [0, 2]\ s, \forall \theta_i, i = 1, \ldots, N \tag{33a}$$

$$\overline{a}(t_i) = \max a(t_i \mid \mathcal{L} \cup \mathcal{T}, \theta) \qquad \forall t_i \in [0, 2]\ s, \forall \theta_i, i = 1, \ldots, N \tag{33b}$$

with $\mathcal{L} \cup \mathcal{T}$ denoting the vertex set of hyper-parameters that bound the basis functions of the imprecise random field and N the number of stochastic realizations of the corresponding random field. As can be noted from this figure, the bounds on the possible displacement profiles are captured perfectly by the bounding of the basis functions at strongly reduced computational cost.

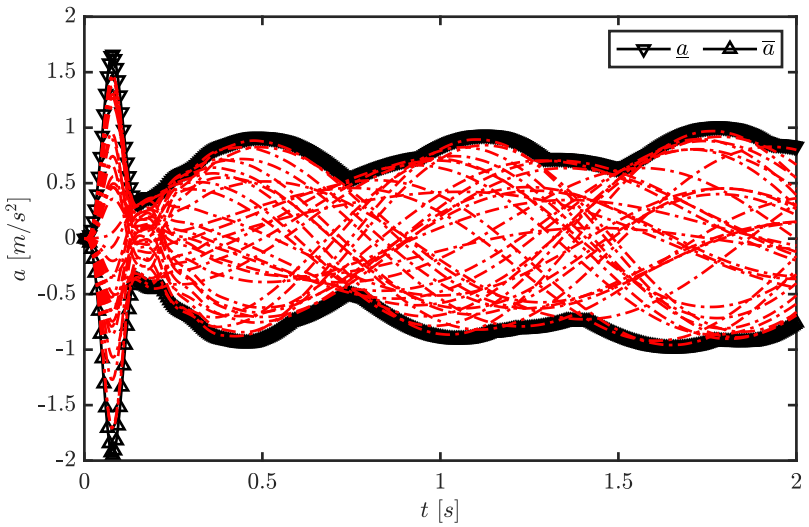

Figure 7: Bounds on the acceleration of the sprung mass, obtained by propagating the hyper-parameter combinations that yield the bounds on the basis functions (in black), as well as extremum-yielding realizations of the Sobol-set simulation (in red).

Figure 8 shows the fitted empirical cumulative distribution functions that are obtained by only propagating those realizations in $\mathcal{H}$ that bound the basis functions of the random field, as well as the result of propagating the Sobol set at time instance $t = 0.085$ s and $t = 1.5$ s. It can be seen that propagating the bounds on the basis functions indeed yields the exact bounds on the imprecise

probabilistic description of the acceleration profile.

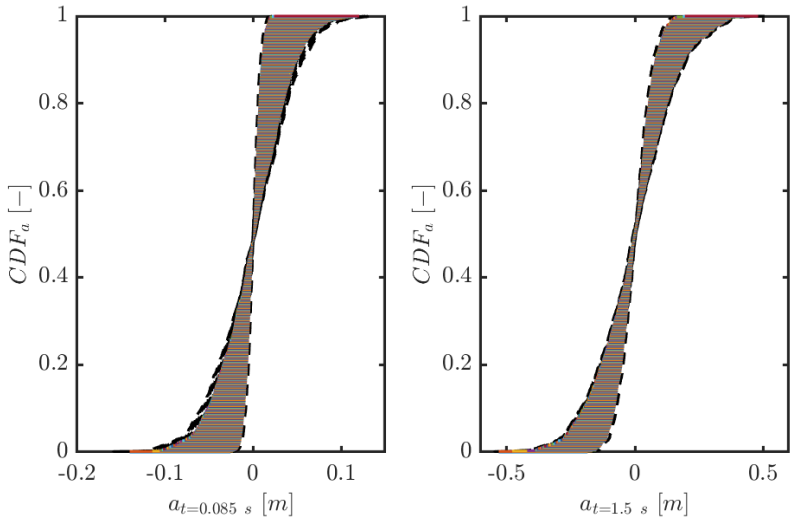

Figure 8: Bounds on the cumulative distribution function of the acceleration profile, as well as the values that are obtained by propagating an imprecise random field by a Sobol set on the hyper-parameters.

The interval on the maximal stroke during the simulated time period (i.e., the relative displacement between the sprung and unsprung mass of the car) is $[4.453e-05; 0.00901]$ m in case only those parameters in $\mathcal{H}$ that yield the bounds on the basis functions are propagated, and $[4.91e-05; 0.00794]$ m when a large-space filling design between the intervals on those parameters is propagated. As such, even when very large bounds are imposed on the uncertain road profile, the proposed methodology is able to give an exact estimate of the bounds on selected quantities of interest of the car dynamics.

From this example, it is clear that an analyst can efficiently compute the bounds on possible comfort indicators of the car suspension, taking into account a large set of possible road topologies. As such, in stead of starting from a predefined road profile, the presented approach enables the assessment of the suspension quality taking into account the impreciseness and randomness in the definition of a road profile.

7. Conclusions

The definition of covariance kernels and their parameters is often performed based on limited data or the engineering judgement of the analyst. To overcome this possible bias, this paper presents an approach to model and simulate Gaussian random fields using the Karhunen-Loève expansion with imprecise covariance kernels. The problem is approached from an interval standpoint, and an iterative procedure is proposed to generate a set of complete $\mathcal{L}_2$ bases that effectively bound the realizations of the imprecise random field. A discussion on when such approach is applicable is included, and specifically focussed on transient dynamic problems. Also an approach to deal with potential eigenfunction cross-over, which inevitably occurs during the determination of the bounds on the realizations, is adapted from structural dynamics and applied to this context. A case study consisting of a linear oscillator, subjected to an excitation that is modeled as a random field with imprecise covariance kernel is included to illustrated the presented ideas. Furthermore, the dynamics of a car suspension while driving over a road that is modeled as an imprecise random field is studied. It is shown that the method is indeed capable of efficiently and effectively computing the bounds on stochastic quantities of interest, such as e.g., the probability of failure or cumulative density function of the response, given the imprecision in the random field input. However, certain monotonicity assumptions need to be fulfilled for the method to provide the exact bounds. Future work will therefore focus on relaxing this need for complete monotonicity.

Acknowledgement

Matthias Faes is a post-doctoral researcher of the Research Foundation Flanders (FWO) under grant number 12P3519N.

References

[1] D. Moens, D. Vandepitte, Recent advances in non-probabilistic approaches for non-deterministic dynamic finite element analysis, Archives of Com-

putational Methods in Engineering 13 (3) (2006) 389–464. doi:10.1007/BF02736398.

[2] M. Faes, M. Broggi, E. Patelli, Y. Govers, J. Mottershead, M. Beer, D. Moens, A multivariate interval approach for inverse uncertainty quantification with limited experimental data, Mechanical Systems and Signal Processing 118 (2019) 534–548. doi:10.1016/j.ymssp.2018.08.050.

[3] M. Faes, D. Moens, Recent trends in the modeling and quantification of non-probabilistic uncertainty, Archives of Computational Methods in Engineeringdoi:10.1007/s11831-019-09327-x.

[4] W. Xiaojun, Q. Zhiping, Interval finite element analysis of wing flutter, Chinese Journal of Aeronautics 21 (2) (2008) 134–140.

[5] M. Modares, S. Venkitaraman, Reliable condition assessment of structures using hybrid structural measurements and structural uncertainty analyses, Structural Safety 52 (2015) 202–208.

[6] L. Farkas, D. Moens, S. Donders, D. Vandepitte, Optimisation study of a vehicle bumper subsystem with fuzzy parameters, Mechanical Systems and Signal Processing 32 (2012) 59–68.

[7] A. Balu, B. Rao, High dimensional model representation based formulations for fuzzy finite element analysis of structures, Finite Elements in Analysis and Design 50 (2012) 217–230.

[8] B. Wu, W. Gao, D. Wu, C. Song, Probabilistic interval geometrically nonlinear analysis for structures, Structural Safety 65 (2017) 100 – 112. doi:http://dx.doi.org/10.1016/j.strusafe.2017.01.002.

[9] Z. Qiu, Z. Zhang, Crack propagation in structures with uncertain-but-bounded parameters via interval perturbation method, Theoretical and Applied Fracture Mechanics 98 (2018) 95–103. doi:10.1016/j.tafmec.2018.09.009.

[10] A. Sofi, E. Romeo, O. Barrera, A. Cocks, An interval finite element method for the analysis of structures with spatially varying uncertainties, Advances in Engineering Software 128 (November 2018) (2019) 1–19. doi:10.1016/j.advengsoft.2018.11.001.

[11] W. Verhaeghe, W. Desmet, D. Vandepitte, D. Moens, Interval fields to represent uncertainty on the output side of a static FE analysis, Computer Methods in Applied Mechanics and Engineering 260 (0) (2013) 50–62. doi:10.1016/j.cma.2013.03.021.

[12] M. Faes, D. Moens, Identification and quantification of spatial interval uncertainty in numerical models, Computers and Structures 192 (2017) 16–33. doi:10.1016/j.compstruc.2017.07.006.

[13] A. Sofi, Structural response variability under spatially dependent uncertainty: Stochastic versus interval model, Probabilistic Engineering Mechanics 42 (2015) 78–86. doi:10.1016/j.probengmech.2015.09.001.

[14] A. Sofi, G. Muscolino, I. Elishakoff, Static response bounds of Timoshenko beams with spatially varying interval uncertainties, Acta Mechanica 226 (11) (2015) 3737–3748. doi:10.1007/s00707-015-1400-9.

[15] M. Faes, D. Moens, Multivariate dependent interval finite element analysis via convex hull pair constructions and the extended transformation method, Computer Methods in Applied Mechanics and Engineering 347 (2019) 85–102.

[16] M. Götz, W. Graf, M. Kaliske, Enhanced uncertain structural analysis with time- and spatial-dependent (functional) fuzzy results, Mechanical Systems and Signal Processing 119 (2019) 23–38. doi:10.1016/j.ymssp.2018.08.041.
URL https://www.scopus.com/inward/record.uri?eid=2-s2.0-85053812998{&}doi=10.1016{%}2Fj.ymssp.2018.08.041{&}partnerID=40{&}md5=d1d837bf3a1b5b9551a27d345a7add88

[17] E. H. Vanmarcke, M. Grigoriu, Stochastic Finite Element Analysis of Simple Beams, Journal of Engineering Mechanics 109 (5) (1983) 1203–1214. doi:10.1061/(ASCE)0733-9399(1983)109:5(1203).

[18] D. Savvas, G. Stefanou, Determination of random material properties of graphene sheets with different types of defects, Composites Part B: Engineering 143 (2018) 47–54. doi:10.1016/j.compositesb.2018.01.008. URL https://www.scopus.com/inward/record.uri?eid=2-s2.0-85041729297{&}doi=10.1016{%}2Fj.compositesb.2018.01.008{&}partnerID=40{&}md5=fef4fca3c90d29f0161f34ea96bf63e5

[19] M. Tian, D. Q. Li, Z. J. Cao, K. K. Phoon, Y. Wang, Bayesian identification of random field model using indirect test data, Engineering Geology 210 (2016) 197–211. doi:10.1016/j.enggeo.2016.05.013.

[20] S. Das, R. Ghanem, S. Finette, Polynomial chaos representation of spatio-temporal random fields from experimental measurements, Journal of Computational Physics 228 (23) (2009) 8726–8751. doi:10.1016/j.jcp.2009.08.025.

[21] D. M. Do, W. Gao, C. Song, M. Beer, Interval spectral stochastic finite element analysis of structures with aggregation of random field and bounded parameters, International Journal for Numerical Methods in Engineering 108 (10) (2016) 1198–1229. doi:10.1002/nme.5251.

[22] D. Wu, W. Gao, Hybrid uncertain static analysis with random and interval fields, Computer Methods in Applied Mechanics and Engineering 315 (2017) 222–246. doi:10.1016/j.cma.2016.10.047.

[23] J. Zheng, Z. Luo, C. Jiang, J. Gao, Robust topology optimization for concurrent design of dynamic structures under hybrid uncertainties, Mechanical Systems and Signal Processing 120 (2019) 540–559. doi:10.1016/j.ymssp.2018.10.026.

[24] M. Faes, G. D. Sabyasachi, D. Moens, Hybrid spatial uncertainty analysis for the estimation of imprecise failure probabilities in Laser Sintered PA-12 parts, Computers & Mathematics with Applications doi:10.1016/j.camwa.2018.08.056.

[25] D. Charmpis, G. Schuëller, M. Pellissetti, The need for linking micromechanics of materials with stochastic finite elements: A challenge for materials science, Computational Materials Science 41 (1) (2007) 27 – 37. doi:https://doi.org/10.1016/j.commatsci.2007.02.014.

[26] J. Ching, K.-K. Phoon, Impact of Autocorrelation Function Model on the Probability of Failure, Journal of Engineering Mechanics 145 (1) (2019) 04018123. doi:10.1061/(ASCE)EM.1943-7889.0001549.
URL http://ascelibrary.org/doi/10.1061/{%}28ASCE{%}29EM.1943-7889.0001549

[27] D. C. Charmpis, G. I. Schuëller, M. F. Pellissetti, The need for linking micromechanics of materials with stochastic finite elements: a challenge for materials science, Computational Materials Science 41 (1) (2007) 27–37.

[28] W. Betz, I. Papaioannou, D. Straub, Numerical methods for the discretization of random fields by means of the Karhunen-Loeve expansion, Computer Methods in Applied Mechanics and Engineering 271 (2014) 109–129. doi:10.1016/j.cma.2013.12.010.

[29] M. Beer, S. Ferson, V. Kreinovich, Imprecise probabilities in engineering analyses, Mechanical Systems and Signal Processing 37 (1-2) (2013) 4–29. doi:10.1016/j.ymssp.2013.01.024.

[30] P. Wei, J. Song, S. Bi, M. Broggi, M. Beer, Z. Lu, Z. Yue, Non-intrusive stochastic analysis with parameterized imprecise probability models: I. performance estimation, Mechanical Systems and Signal Processing 124 (2019) 349 – 368. doi:https://doi.org/10.1016/j.ymssp.2019.01.058.

[31] W. Verhaeghe, W. Desmet, D. Vandepitte, D. Moens, Random field expansion with interval correlation length using interval fields, in: Eurodyn 2011, Leuven, 2011, pp. 2662–2667.

[32] M. M. Dannert, A. Fau, R. M. Fleury, M. Broggi, U. Nackenhorst, M. Beer, A probability-box approach on uncertain correlation lengths by stochastic finite element method, PAMM 18 (1) (2018) e201800114. arXiv:https://onlinelibrary.wiley.com/doi/pdf/10.1002/pamm.201800114, doi:10.1002/pamm.201800114.

[33] W. Gao, D. Wu, K. Gao, X. Chen, F. Tin-loi, Structural reliability analysis with imprecise random and interval fields 55 (2018) 49–67. doi:10.1016/j.apm.2017.10.029.

[34] P. Spanos, R. Ghanem, Stochastic finite element expansion for random media, Journal of engineering mechanics 115 (5) (1989) 1035–1053.

[35] M. Grigoriu, Simulation of stationary non-gaussian translation processes, Journal of Engineering Mechanics 124 (2) (1998) 121–126. doi:10.1061/(ASCE)0733-9399(1998)124:2(121).

[36] R. Ghanem, Ingredients for a general purpose stochastic finite elements implementation, Computer Methods in Applied Mechanics and Engineering 168 (1) (1999) 19–34.

[37] K. K. Phoon, H. W. Huang, S. T. Quek, Simulation of strongly non-Gaussian processes using Karhunen-Loeve expansion, Probabilistic Engineering Mechanics 20 (2) (2005) 188–198. doi:10.1016/j.probengmech.2005.05.007.

[38] M. Beer, I. A. Kougioumtzoglou, E. Patelli, Emerging Concepts and Approaches for Efficient and Realistic Uncertainty Quantification, in: Maintenance and Safety of Aging Infrastructure, Structures & Infrastructures Series, CRC Press, 2014, pp. 121–161. doi:doi:10.1201/b17073-6.

[39] R. G. Ghanem, P. D. Spanos, Stochastic Finite Elements: A Spectral Approach, Springer-Verlag New York, Inc., New York, NY, USA, 1991.

[40] J. L. Beck, S.-K. Au, Bayesian updating of structural models and reliability using markov chain monte carlo simulation, Journal of Engineering Mechanics 128 (4) (2002) 380–391.

[41] M. Hladik, D. Daney, E. P. Tsigaridas, M. Hladik, D. Daney, E. P. Tsigaridas, Bounds on eigenvalues and singular values of interval matrices To cite this version : HAL Id : inria-00370603 Bounds on eigenvalues and singular values of interval matrices.

[42] A. Deif, The Interval Eigenvalue Problem, ZAMM - Journal of Applied Mathematics and Mechanics / Zeitschrift für Angewandte Mathematik und Mechanik 71 (1) (1991) 61–64. arXiv:arXiv:1011.1669v3, doi:10.1002/zamm.19910710117.

[43] F. Gioia, C. N. Lauro, Principal component analysis on interval data, Computational Statistics 21 (2) (2006) 343–363. doi:10.1007/s00180-006-0267-6.

[44] N. P. Seif, S. Hashem, A. S. Deif, Bounding the Eigenvectors for Symmetric Interval Matrices, ZAMM - Journal of Applied Mathematics and Mechanics / Zeitschrift fur Angewandte Mathematik und Mechanik 72 (3) (1992) 233–236. doi:10.1002/zamm.19920720313.

[45] N. S. Nedialkov, V. Kreinovich, S. A. Starks, Interval arithmetic, affine arithmetic, Taylor series methods: Why, what next?, Numerical Algorithms 37 (1-4 SPEC. ISS.) (2004) 325–336. doi:10.1023/B:NUMA.0000049478.42605.cf.

[46] G. Muscolino, A. Sofi, Stochastic analysis of structures with uncertain-but-bounded parameters via improved interval analysis, Probabilistic Engineering Mechanics 28 (2012) 152–163. doi:10.1016/j.probengmech.2011.08.011.

[47] M. Hanss, The extended transformation method for the simulation and analysis of fuzzy-parameterized models, International Journal of Uncertainty, Fuzziness and Knowledge-Based Systems 11 (06) (2003) 711–727. doi:10.1142/S0218488503002491.

[48] H. Zhang, R. L. Mullen, R. L. Muhanna, Interval monte carlo methods for structural reliability, Structural Safety 32 (3) (2010) 183 – 190. doi:https://doi.org/10.1016/j.strusafe.2010.01.001.

[49] G. Blatman, B. Sudret, Adaptive sparse polynomial chaos expansion based on least angle regression, Journal of Computational Physics 230 (6) (2011) 2345 – 2367. doi:http://dx.doi.org/10.1016/j.jcp.2010.12.021.

[50] J. Mottershead, M. Friswell, Model updating in structural dynamics: a survey, Journal of sound and vibration 167 (2) (1993) 347–375.

[51] M. De Munck, Efficient optimisation approaches for interval and fuzzy finite element analysis, Ph.D. thesis, PhD thesis, faculty of Engineering KU Leuven (2009).

[52] P. D. Spanos, M. Beer, J. Red-Horse, Karhunen-loève expansion of stochastic processes with a modified exponential covariance kernel, Journal of Engineering Mechanics 133 (7) (2007) 773–779. doi:10.1061/(ASCE)0733-9399(2007)133:7(773).